www.czasopisma.pan.pl PAN POLSKA AKADEMIA NAUK www.journals.pan.pl

A R C H I V E S O F M E T A L L U R G Y A N D M A T E R I A L S

Volume 56 2011 Issue 2

DOI: 10.2478/v10172-011-0056-2

D. KUC*, J. GAWĄD**

MODELLING OF MICROSTRUCTURE CHANGES DURING HOT DEFORMATION USING CELLULAR AUTOMATA

MODELOWANIE ZA POMOCĄ AUTOMATÓW KOMÓRKOWYCH ZMIAN MIKROSTRUKTURY PODCZAS ODKSZTAŁCENIA NA GORĄCO

The paper is focused on an application of the cellular automata (CA) method to description of microstructure changes in continuous deformation condition. The model approach consists of Cellular Automata model of microstructure development and the thermal-mechanical finite element (FE) code. Dynamic recrystallization phenomenon is taken into account in 2D CA model which takes advantage of explicit representation of microstructure, including individual grains and grain boundaries. Flow stress is the main material parameter in mechanical part of FE and is calculated on the basis of average dislocation density obtained from the CA model. The results obtained from the model were validated with the experimental data. In the present study, austenitic steel X3CrNi18-10 was investigated. The examination of microstructure for the initial and final microstructures was carried out, using light microscopy, transmission electron microscopy and EBSD technique. Compression forces were recorded during the tests and flow stresses were determined using the inverse method.

Keywords: modelling, cellular automata, austenitic steel, flow stress, microstructure

W artykule przedstawiono model, który opisuje zmiany struktury w warunkach ciągłego odkształcenia z wykorzystaniem automatów komórkowych. Opracowane rozwiązanie wykorzystuje połączenie modelu automatów komórkowych (ang. Cellular Automata, CA) zmian mikrostruktury i kodu elementów skończonych rozwiązującego problem termomechaniczny. Do opracowania modelu zmian mikrostruktury wykorzystano dwuwymiarową siatkę automatów komórkowych. Model zmian naprężenia uplastyczniającego bazuje na średniej gęstości dyslokacji wyliczonej poprzez homogenizację gęstości dyslokacji w siatce automatów komórkowych. Opracowany model zweryfikowano w oparciu o wyznaczone krzywe płynięcia dla stali austenitycznej X3CrNi18-10 i badania mikrostruktury z wykorzystaniem mikroskopii świetlnej, transmisyjnej mikroskopii elektronowej oraz techniki EBSD. Naprężenie uplastyczniające zostało wyznaczone w oparciu o metodę obliczeń odwrotnych na podstawie danych uzyskanych z prób osiowosymetrycznego ściskania.

1. Introduction

Over the last ten years the models of recrystallization phenomena have become extended by several groups of approaches based on direct representation of microstructure. The interactions between individual grains and inside grain interiors can be simulated using the methods such as Monte Carlo (MC), Cellular Automata (CA), Phase Field (PF), Vertex Method and others (a review can be found e.g. in [1]). The key concept of these methods is to represent a microstructure in a suitable computational lattice by a spatial discretization in two or three dimensions. An initial representation of the microstructure is commonly generated using normal grain growth algorithm. In previous studies, the grain size was considered as a major parameter describing the microstructure represented in the lattice. Minor emphasis was put on grain misorientation distribution in the initial microstructure, despite the initial misorientation affects the recrystallization process to a large extent. In particular, the nucleation process is influenced by the presence of specific types of grain boundaries. The paper is focused on application of a multi-scale 2D method in hot forming. Modern Cellular Automata models of recrystallization phenomena take into account the influence of grain misorientation on both the nucleation and the growth of new grains. Therefore, correctness of the assumptions on misorientation between the grains is crucial for the overall reliability of the CA simulation.

Over the last decade several successful applications

* SILESIAN UNIVERSITY OF TECHNOLOGY, FACULTY OF MATERIALS SCIENCE AND METALLURGY, 40-019 KATOWICE, 8 KRASIŃSKIEGO STR., POLAND

** AGH UNIVERSITY OF SCIENCE AND TECHNOLOGY, FACULTY OF METAL ENGINEERING AND INDUSTRIAL COMPUTER SCIENCE, 30-049 KRAKÓW, 30 MICKIEWICZA AV., POLAND

of the CA in simulation of dynamic recrystallization can be found in the literature, e.g. [2–5]. The CA method offers a reasonable balance between its computational simplicity and ability to provide quantitative results. However, the boundary conditions that are imposed in the CA simulation of dynamic recrystallization are usually simplistic. For example, constant temperature and strain rate are typically assumed throughout the entire deformation process. One can make more realistic assumptions on the boundary conditions by combining the CA method with a macroscopic model of deformation process. A specific coupling of the CA with the FE method is referred to as a CAFE approach [6]. The CAFE consists of Cellular Automata model of microstructure development and the thermal-mechanical Finite Element (FE) macroscopic simulation. If a hot forming process is considered, the CAFE model can take into account the recrystallization phenomena. For example, the dynamic recrystallization phenomenon can be modelled by the CA, which takes advantage of an explicit representation of the microstructure, dealing with individual grains, grain boundaries and inertia of the grains. Flow stress is the main material parameter in the FE mechanical part of the CAFE and is calculated on the basis of average dislocation density obtained from the CA model. Some previously published results that were obtained using this approach appear very encouraging, see [5, 7].

In the present study, austenitic X3CrNi18-10 steel was investigated. This specific material was selected to avoid phase transformation in the lower range of temperatures. The samples were subjected to an axisymmetrical hot compression test. The results attained from the CA model were validated with the experimental data.

2. Cellular automata model of recrystallization

In general, any Cellular Automaton is described by a quadruplet: <L, S, F, N>, where L is a lattice (spatial ordering) of the cells, S is a state of the cell, F is a state transition rule governing an evolution of the state in consecutive time steps and N is a definition of neighbourhood describing a range of local interactions between the cells. In the current work the CA is used for modelling of the microstructure and dislocation density evolution. The 2D CA lattice of cells represents a cross section of a three dimensional microstructure and reproduces topological relations between the grains. These relations include length of the grain boundaries (GB) as well as selected properties of the boundary, e.g. its misorientation. Periodic boundary conditions are imposed at the outer edges of the lattice. The pseudohexagonal neighbourhood provides a context for the state transition rule as described in [1]. The state of each CA cell is described by three state variables: 1) local dislocation density ρ, 2) distance variable x that controls migration of GB, 3) assignment to a grain.

The grains in the system are modelled by Distant Neighbourhoods (DN). Detailed motivation for the concept of DN and its description are presented in [3]. Every instance of the DN keeps an internal state which comprises: 1) orientation of a grain ϕ, 2) average dislocation density inside the grain ρ_{gr} and 3) number of cells belonging to the grain. The evolution of average dislocation density is calculated separately for each grain in the computational lattice, according to the differential equation in which the first term describes a hardening of material, while the second expresses the influence of a dynamic recovery [8]:

$$\frac{d\rho_{gr}}{dt} = k_1 \frac{\dot{\varepsilon}}{bl} - k_2 \dot{\varepsilon}^m \exp\left(\frac{Q_s}{RT}\right)\rho_{gr} \tag{1}$$

where t is time, b is Burgers vector, l is a mean free path of dislocation, $\dot{\varepsilon}$ is strain rate, Q_s is activation energy of self-diffusion, T is temperature, R is gas constant and k_1, k_2, m are parameters.

The equation (1) is solved numerically using the fourthorder Runge-Kutta method. The average dislocation density calculated in the previous time step is used as an initial condition for the subsequent step. Once the increment of dislocation density ρ_{gr} is calculated, the ρ variable in the CA cells belonging to the grain is updated using a nondeterministic algorithm ensuring homogeneous distribution of dislocation density inside the grain.

Nucleation of new grains and their successive growth is reproduced in the model by the state transition rules. Despite the rules itself are deterministic, the result of their application is not deterministic, due to quasi-random neighbourhood definition and dislocation density distribution within the CA lattice. The rule describing the nucleation of new grains is based on critical dislocation density criterion. The nucleus appears if the cell is located at the GB and the dislocation density in the cell reaches a critical value ρ_c, according to equation derived from [9]:

$$\rho_{cr} = \left(\frac{20}{3b\tau^2} \frac{\dot{\varepsilon}(\varepsilon)}{l(\varepsilon, D)} \frac{\gamma(\theta)}{M(\theta, T)}\right)^{1/3} \tag{2}$$

where γ is GB energy, M is GB mobility, τ is average energy of dislocation line, θ is GB misorientation angle calculated as $\theta = |\phi_1 - \phi_2|$, where ϕ_1 and ϕ_2 are orientation variables of grains on both sides of GB. Due to both heterogeneous distribution of dislocation density within the grains as well as the misorientation dependence of ρ_c, it is possible to select a subset of sites in the CA lattice in which the nuclei may appear. The current model allows the nuclei to appear rather due to actual process

conditions than due to a premise on an *a priori* known nucleation rate. Once the CA cell is selected as a nucleus, the dislocation density in the cell is set to ρ_{DRX} and new instance of DN is created. A random orientation is assigned to a newly created grain.

The further growth of recrystallized grains is described by the second rule, which may increment the state variable x. In principle, this rule is based on the GB velocity, which is a product of GB mobility M and the driving force for growth F:

$$\Delta x = \frac{\alpha}{\sqrt{S}} M F \Delta t \tag{3}$$

where Δt is length of the time step, S is area of the 2D CA cell and α is a scaling factor.

The distance variable is updated by using a threshold function, which ensures $0 \leqslant x \leqslant 1$. The GB mobility is assumed to depend on GB misorientation angle and the temperature of the system. Mobility of an arbitrary GB is limited by a mobility of high angle boundary [10]:

$$M(\theta, T) = M_0 \exp\left(\frac{-Q}{kT}\right)\left[1 - \exp\left(-B\frac{\theta}{\theta_m}\right)^n\right] \tag{4}$$

where M_0 is a pre-exponential factor, Q is activation enthalpy for GB motion, k is Boltzmann constant, T is temperature, θ_m – misorientation angle for high angle GB and B, n are coefficients.

Grain boundary energy γ is calculated according to the Read–Shockley equation [10]:

$$\gamma(\theta) = \gamma_m \frac{\theta}{\theta_m}\left(1 - \ln\frac{\theta}{\theta_m}\right) \tag{5}$$

where γ_m is GB energy for high angle boundaries exceeding misorientation θ_m.

An equation describing a driving force for grain growth is based on an assumption that the grain boundaries migrate mainly due to a difference in stored energy on both sides of the boundary. Therefore, the effect of a difference in dislocation density across the GB prevails over any other factors (e.g. curvature of the boundary) that may control the migration of the GB [1]. The driving force is calculated according to the difference in dislocation density between the current CA cell belonging to the recrystallized grain and the i^{th} neighbouring cell belonging to the deformed matrix:

$$F = \frac{\pi D^2 \tau}{M} \sum_{i=1}^{R} (\rho_i - \rho) \tag{6}$$

where R is a number of neighbouring cells belonging to other grains, D is the equivalent grain size.

The CA model of DRX provides the macroscopic mechanical FE with the flow stress. In the current model the flow stress is calculated by homogenizing the dislocation density over the whole CA lattice. The homogenization procedure delivers an average dislocation density inside a representative volume of material that is connected to a given FE integration point. Subsequently, the average dislocation density is used for calculation of the flow stress, which is an essential material parameter for the FE model:

$$\sigma_f(t, \dot{\varepsilon}, T) = \alpha \mu b \sqrt{\rho_{CA}(t, \dot{\varepsilon}, T)} \tag{7}$$

where α is a coefficient, μ is shear modulus, b is a length of the Burgers vector, t is time and ρ_{CA} is the average dislocation density in the CA lattice.

3. Experimental procedure

An austenitic steel X3CrNi18-10 was investigated. This steel grade does not undergo a phase transformation in a lower range of temperatures, which simplifies a quantitative characterization of the microstructure. The steel was used for a preparation of samples for the axisymmetrical hot compression tests on a GLEEBLE 3800 simulator. The compression tests were conducted at temperature in range 900-1100°C and a strain rate of 0.001-0.1s^{-1}. The samples were rapidly quenched after the deformation in order to freeze the microstructure. The metallographic investigation was performed on an OLYMPUS GX51 light microscope. Structural studies were conducted on longitudinal sections of the samples. Misorientation maps were elaborated in that case on a high-resolution scanning electron microscope. Processing of the results (i.e. obtaining maps, distributions, etc.) was performed using TSL OIM Data Collection 5. As a result of the examination, structural maps were obtained for the steel in its initial state after soaking and after hot plastic deformation, which allowed one to determine distributions of misorientation angles and grain size distributions in the samples.

The examination of the substructure was carried out by means of a JEOL 100B transmission microscope of accelerating voltage of 100 kV. The mean dislocation density was calculated by use of a method based on counting the inter-section points of a network superimposed over the micrograph with dislocation lines. The dislocation density ρ as calculated for the thin foils according to the relation [11]:

$$\rho = \frac{x(n_1/l_1 + n_2/l_2)}{t} \tag{8}$$

where x is a coefficient which defines the fraction of invisible dislocations with Burgers vectors *a/<111>* for the A1 structure [11]:
x = 2 for image of dislocations observed in (111) reflex,

x = 1,5 for image of dislocations observed in (200) reflex,
x = 1,5 for image of dislocations observed in (220) reflex,

$l_{1(2)}$ is the total length of the horizontal (vertical) lattice lines $n_{1(2)}$ is a number of intersections of the horizontal (vertical) lattice with dislocations, and t is the thickness of the foil.

The thickness of the foil in the investigated areas can be approximately calculated following the formula:

$$t = n \cdot \zeta_{hkl} \quad (9)$$

where n is a number of extinction lines; ζ_{hkl} is a value of extinction. The values of extinction ζ_{hkl} can be found in [12]. One should remark that the value of extinction depends on various factors, including chemical composition of the sample. For this reason the value of ζ_{hkl} given in [12] must be considered as a rough estimation of the actual value of extinction for the investigated material.

4. Results

The CA simulation requires an initial representation of the microstructure in the computational lattice. A CA-based algorithm of normal grain growth was used for this purpose. A method that generates initial microstructures bearing resemblance to the initial ones is described in detail elsewhere [3]. The digital microstructure consisted of 100 grains. The generated microstructure resembled the austenitic structure that had been obtained after the heat treatment of the samples. The investigated steel had a diverse grain size with a small number of annealing twins (Fig. 1). The plot of the generated microstructure is shown in Figure 2. The distribution of grain size for the real microstructure of the material is shown in Figure 3a. The Kolmogorow-Smirnow statistical test has confirmed compatibility of grain size distribution in the generated and real microstructure.

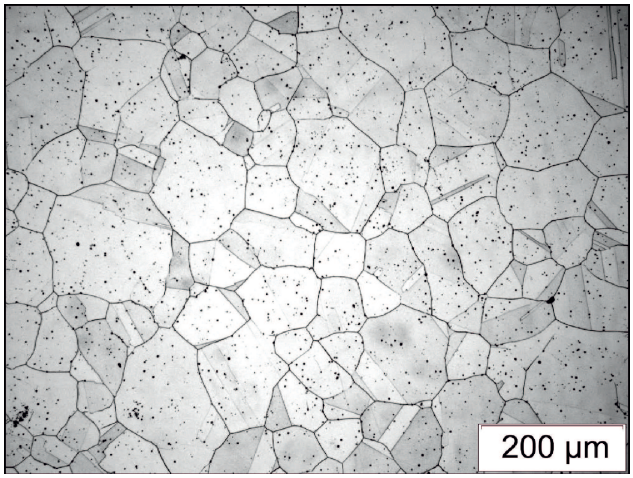

Fig. 1. Microstructures of the investigated steel after solution heat treatment at 1150°C 1h

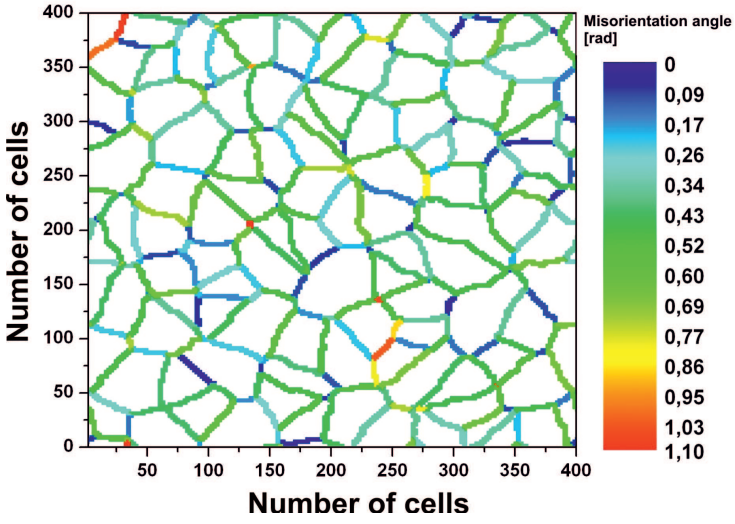

Fig. 2. A generated representation of the austenitic microstructure in the 2D CA lattice. The microstructure consists of 100 grains, misorientation angles of grain boundaries are marked with colour scale

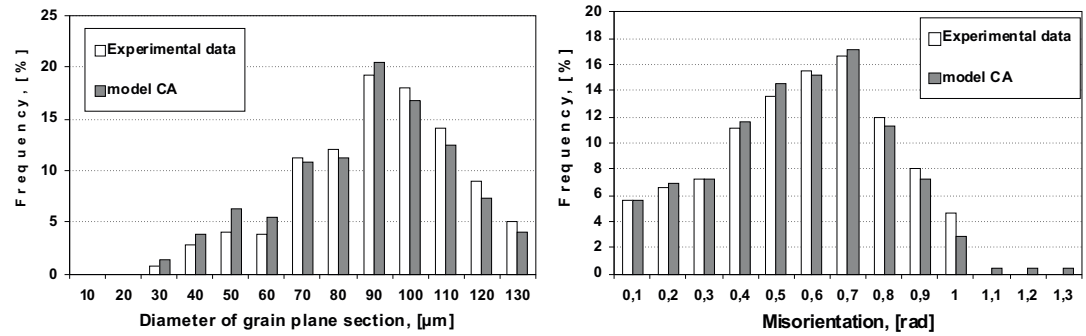

a) b)

Fig. 3. Distribution of average equivalent diameter of grain plane section (a) and misorientation angle (b) as obtained from the experimental data and calculated using the CA model for the sample in the initial state

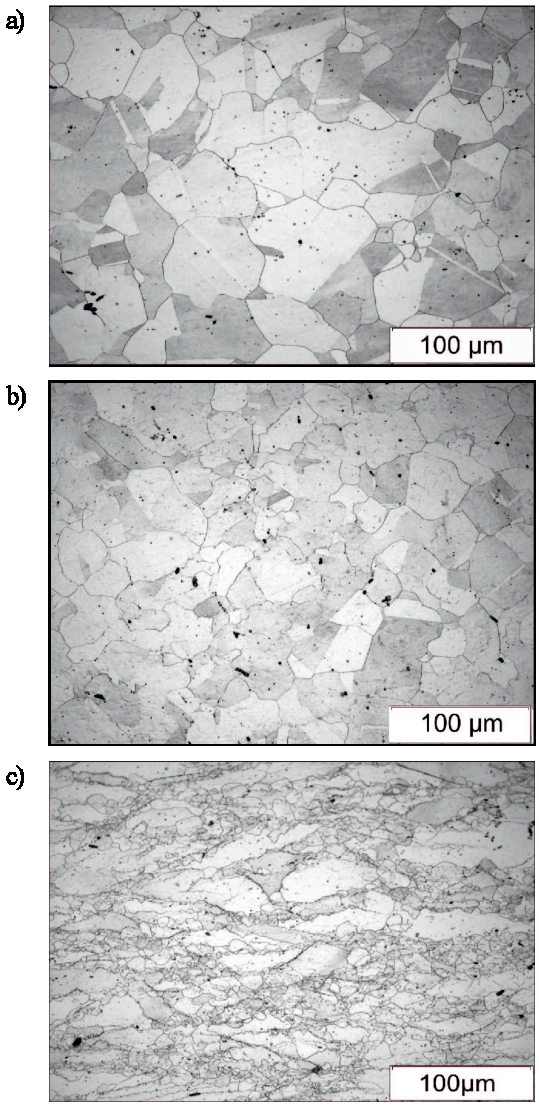

Fig. 4. Typical microstructures after hot deformation of investigated austenitic steel. The samples were subjected to deformation ε= 1 in the following process conditions: a) 1100°C / 0.01 s^{-1}, b) 1100°C / 0.1 s^{-1} and c) 1100°C / 1 s^{-1}. A completely dynamically recrystallized microstructure is observed in Fig. c) while Fig. d) shows a bimodal microstructure

As a result of this procedure, an initial representation of microstructure minimizing the discrepancies between experimental and calculated misorientation is obtained. The comparison of the misorientation angles in the artificial microstructure with the EBSD data is presented in Figure 3b.

For the entire analysed range of deformation rates, substantial changes in the structure were observed, as they were induced by the dynamic recrystallization process. For instance, an entirely dynamically recrystallized microstructure was observed after the deformation at temperature 1100°C at the rate of 0.01 s^{-1} and 0.1 s^{-1} (Fig. 4a, b). After compression at 1100°C / 1 s^{-1} a bimodal structure consisting of recrystallized grains and elongated primary grains was detected (Fig. 4c).

Influence of deformation on the redevelopment process of the microstructure is presented in an EBSD map shown in Figure 5. As the deformation increases, new recrystallized grains gradually appear in the microstructure, initially at corrugated boundaries of primary grains (Fig. 5a), and next, also inside the deformed primary grains (Fig. 5b). Once the deformation reaches a level that corresponds to a steady-state flow, the structure of the steel consists of fine recrystallized grains (Fig. 5c). More detailed study on the development of the microstructure during the hot deformation of the material was presented elsewhere [13].

The parameters of the CA model were determined using the inverse analysis, following the methodology described in [14]. Nelder-Mead simplex method was used as an optimization procedure. The goal function was defined as a square root error between the experimentally determined flow stress and the stress calculated by the CA model according to the equation (7).

The CA model allows one to track an instantaneous state of the microstructure. As it is shown in Figure 6, the CA model makes also possible to plot a spatial distribution of recrystallized grains at successive stages of deformation. Moreover, the CA model enables one to

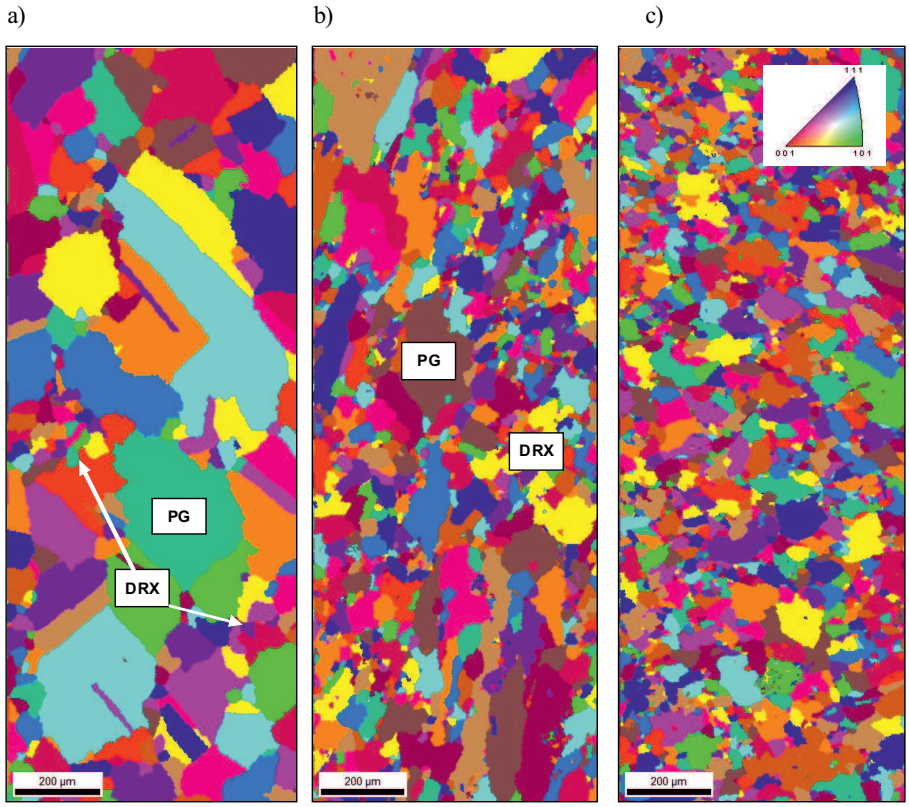

Fig. 5. EBSD microstructure maps after hot deformation at 1000°C and strain rate of 0.01 s^1: a) ε=0.4, b) ε=0.6, c) ε=0.8. DRX – recrystallized grains, PG – elongated primary grain

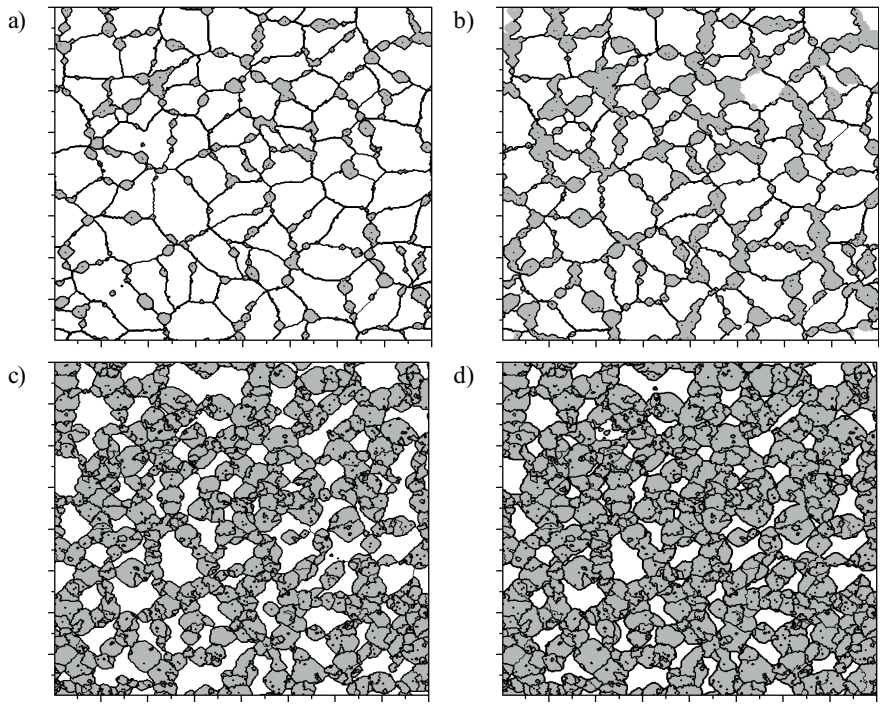

Fig. 6. Evolution of the microstructure predicted by the CA model of DRX at selected stages of recrystallization: a) X_{drx} = 0.15, b) X_{drx} = 0.35 c) X_{drx} = 0.65 and d) X_{drx} = 0.85. Deformation conditions: 1000°C and strain rate of 0.01 s^{-1}. New dynamically recrystallized grains are marked gray, primary grain are denoted by white fields. Grain boundaries are marked with black lines

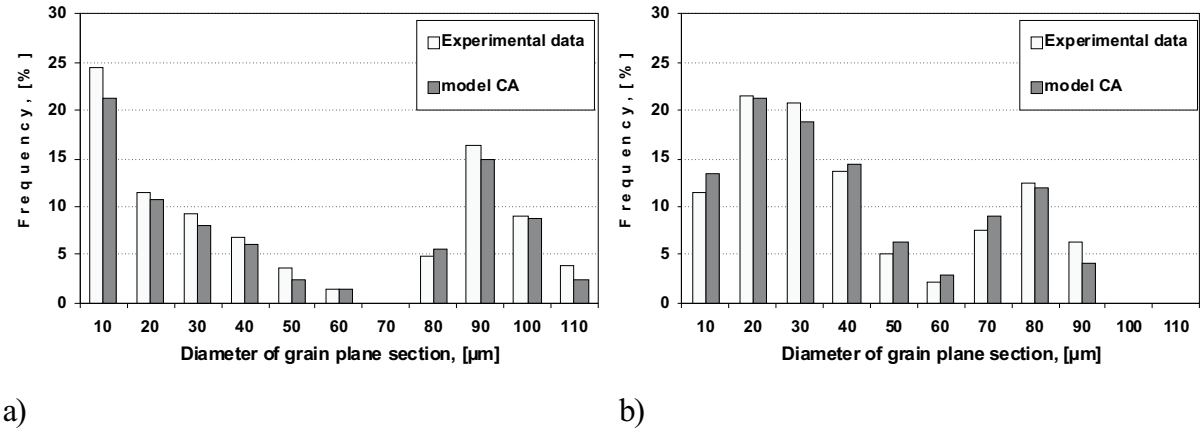

Fig. 7. Distribution of grain size (average equivalent diameter of grain plane section) gathered from the experimental data and calculated using the CA model for sample deformed at the temperature 1000°C with a strain rate 0.01 s^{-1} up to strain: a) ε=0.3, b) ε=0.6

classify the grains observed in the simulated microstructure according to their size. Such classification can be done at requested time steps of simulation, thus the evolution of grain size distribution can be tracked as well. The frequency of occurrence of the grains size in both the simulated and the measured microstructure after deformation at 1000°C at a strain rate of 0.01 s^{-1} up to strain 0.4 and 0.8 are presented in figure 7a and b, respectively. In the current work we decided to remove very small grains from the analysis of the grain size distribution. Those grains correspond to nuclei, which in principle are not revealed in the experimental investigation. For this reason, the grains that consisted of less than two CA cells were filtered out. After the removal, the distribution of the grain diameter calculated by the model is in a good agreement with the experimental measurement. The frequency of occurrence of the GBs characterized by different misorientation angle can be calculated as shown in Fig. 8. The corresponding EBSD measurement of misorientation in the final microstructures is plotted in figure 5c. One may conclude that the model is able to predict very precisely the distribution of misorientation boundaries.

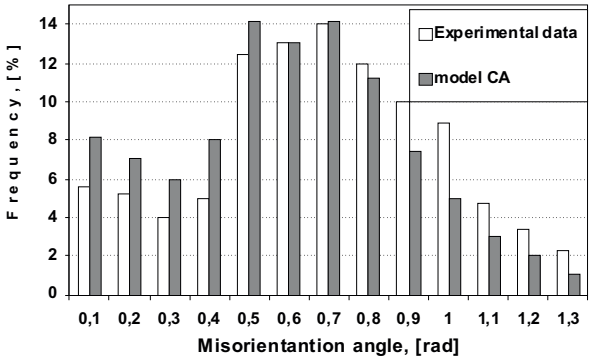

Fig. 8. Distribution of misorientation angle determined from the EBSD data and calculated by means of the CA model for a sample deformed at temperature 1000°C with a rate 0.01 s^{-1} to strain ε =0.8

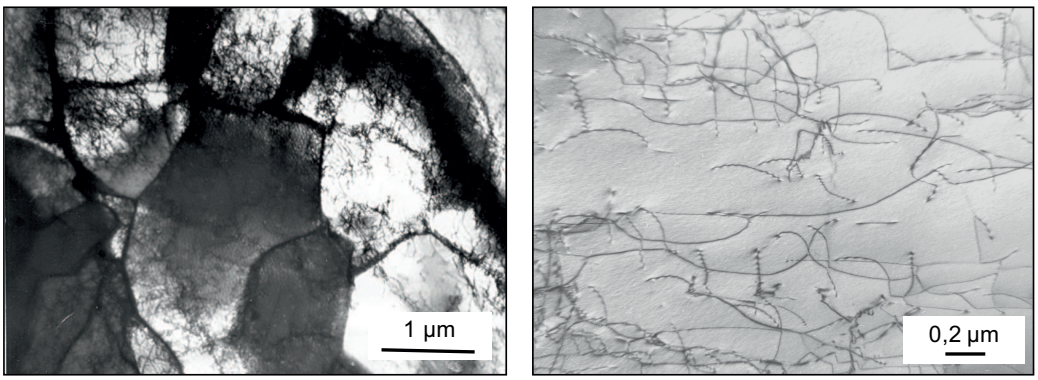

Fig. 9. Substructure after hot deformation at 1000°C/0.01 s^{-1} to strain ε =: a) well-defined subgrain, b) example of an image that was used for determination of the dislocation density

TABLE 1

Grain size (D_{drx}) (average equivalent diameter of grain plane section) and average dislocation density ρ_{DRX} after deformation ε =1 from the experimental data and calculated using the developed CA model

T [°C]	$\dot{\varepsilon}$ [s^{-1}]	D_{drx} [μm]	D_{drx} model CA	$\rho_{DRX}(\varepsilon = 1)$ [m^{-2}]	$\rho_{CA}(\varepsilon = 1)$ model CA
900	0.01	9.1 (partial DRX)	8.2	1.40×10^{14}	1.01×10^{14}
900	0.1	no DRX	–	–	2.10×10^{14}
900	1	no DRX	–	3.41×10^{14}	2.81×10^{14}
1000	0.01	23.1	22.2	2.53×10^{13}	2.95×10^{13}
1000	0.1	12.0 (partial DRX)	12.1	–	8.79×10^{13}
1000	1	11.1 (partial DRX)	10.4	$2{,}17\times10^{14}$	$1{,}81\times10^{14}$
1100	0.01	26.9	28.5	2.21×10^{13}	2.95×10^{13}
1100	0.1	12.4	11.8	–	3.43×10^{13}
1100	1	13.9 (partial DRX)	12.2	5.21×10^{13}	4.22×10^{13}

A substructure that has been formed after the deformation at 1000°C with a strain rate of 0.01 s^{-1} is presented in Figure 9a,b. A number of well-formed subgrains with diversity in the dislocation density can be identified in Figure 9a. An example of the substructure image that was used for estimation of dislocation density is presented in Figure 9b.

Table 1 presents a comparison of the average grain size and the average dislocation density that were obtained from the experimental data and calculated by means of the CA model for various strain rates and temperatures. As it can be seen in this table, the model is capable of predicting the most relevant final characteristics of the microstructure. For example, after the deformation at temperature 1100°C with a stain rate of 0.01 s^{-1}, the average grain diameter calculated by the model is 28.5 μm, which remains in a reasonable quantitative agreement with the experimental measurement (26.9 μm). For the same process conditions, the dislocation density in the simulation reaches approximately the same level as it was found in the experiment. As another example, the CA simulation for deformation at 1000°C and strain rate of 0.01 s^{-1} yields in the dislocation density 2.95×10^{13} m^{-2}, while the experimental measurement of dislocation density resulted in 2.53×10^{13} m^{-2}. An assessment of the remaining cases suggests that the CA model can estimate properly the overall influence of hardening, recovery and dynamic recrystallization on the development of dislocation density. However, one must take cognizance of some limitations in the experimental procedure that was used for determination of the dislocation density. There is also another source of errors due to inaccuracies of material parameters that were used as an input for the CA model. Bearing in mind both origins of errors, we may conclude that the estimations of the dislocation density given by the model and the experiment are in good correspondence.

The calculated flow stresses for selected process conditions and their experimental counterparts are presented in Figure 10. The results of inverse analysis were applied for the calculations. It can be seen that CA model is capable of predicting the flow stress quite precisely for higher strains where the dynamic recrystallization occurs. Nevertheless, some discrepancies are found for the strains below 0.2.

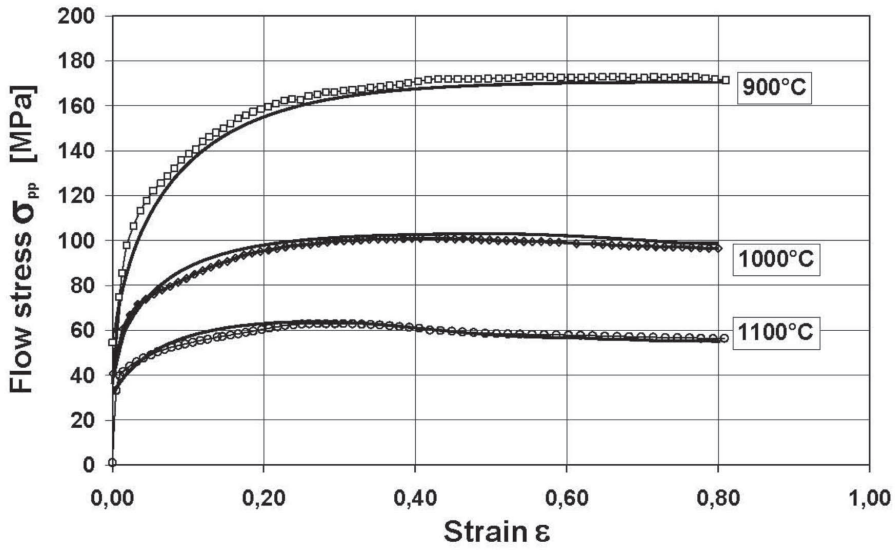

Fig. 10. Flow stress obtained from an inverse analysis [13] of the experimental data (lines with marker) and calculated by the CA model using identified parameters (continuous lines). Uniform strain rate of 0.01 s^{-1} was used in the deformation

5. Conclusion

The Cellular Automata model has been developed to describe the microstructures evolution during the hot deformation of the austenitic steel X3CrNi18-10. The cellular automata model assumes a heterogeneous nucleation: first on the primary grain boundaries and then on the boundaries of deformed recrystallized grains. The model makes use of basic material parameters and it can predict the recrystallization kinetics, grain size and misorientation. If the homogenization technique is applied, the model can deliver the outputs that can be considered as internal variables. For example, the average dislocation density and average grain size evolve throughout the deformation process, but those averaged values originate from an intrinsic evolution of the simulated microstructure. In contrast to the internal variable models, the CA approach is not limited to mean values, but it predicts much richer state of the microstructure. Furthermore, the distributions of these parameters can be derived as well, e.g. distribution of grain size at selected material point.

Experimental verification of the CA model shows good predictive capabilities of the model for austenitic steels. The model is able to predict the evolution of flow stress, grain size and dislocation density. The modelling can be easily extended to other metals subjected to hot deformations.

Acknowledgements

This work was supported by a grant N507 3805 33 from the Polish Ministry of Science and Higher Education, Poland

REFERENCES

[1] M.A. Miodownik, A review of microstructures computer models used to simulate grain growth and recrystallization in aluminum alloys, J. of Light Metals **2**, 125-135 (2002).

[2] R. Ding, X.Z. Guo, Coupled quantitative simulation of microstructural evolution and plastic flow during dynamic recrystallization Acta Mater. **49**, 3163-3168 (2001).

[3] R.L. Goetz, Z. Seetharaman, Modelling dynamic recrystallization using cellular automata, Scripta Mater. **38**, 405-410 (1998).

[4] Ch. Zheng, N. Xiao, D. Li, Y. Li, Microstructure prediction of the austenite recrystallization during multi-pass, Comp. Mat. Sci. **44**, 507-514 (2008).

[5] D. Kuc, J. Gawąd, M. Pietrzyk, Multiscale CAFE Modelling of Dynamic Recrystallization, Materials Science Forum **638-642**, 2567-2572 (2010).

[6] S. Das, E.J. Palmiere, I.C. Howard, CAFE: a tool for modeling thermomechanical processes. Proc conf. Thermomech. Processing: Mechanics, Microstructure and Control, Eds. E. J. Palmiere, M. Mahfouf, C. Pinna, Sheffield, 296-301 (2002).

[7] J. Gawąd, D. Kuc, Application of Cellular Automata and Particle Swarm Optimization methods to identification of initial microstructure representation, Hutnik Wiadomości – Hutnicze **8**, 568-600 (2009).

[8] H. Mecking, U.F. Kocks, Kinetics of Flow and Strain-Hardening, Acta Metall. **29**, 1865-1875 (1981).

[9] W. Roberts, B. Ahlblom, A nucleation criterion for dynamic recrystallization during hot working Acta Metall. **29**, 801-813 (1978).

[10] F.J. Humphreys, A unified theory of recovery, recrystallization and grain growth, based on the stability

and growth of cellular microstructures, Acta Mater. **45**, 4231-4240 (1997).

[11] H.J. K l a a r, P. S c h w a a b, W. Ö s t e r l e, Ringversuch zur quantitativen Ermittlung der Versetzungsdichte im elektronen mikroskop, Prakt. Metallogr. **29**, 3-25 (1992).

[12] A.K. H e a d, P. H u m b l e, L.M. C l a r e b r o u g h t, A.J. M o r t o n, C.T. F o r w o o d, Computed Electron Micrographs and Defect Identification; University of Melbourne, Australia (1973).

[13] G. N i e w i e l s k i, D. K u c, Structure and properties of high – alloy hot deformed steels, Hadasik E. Schindler I. Plasticity of Metallic Materials, Publishers of the Silesian University of Technology, 199-221 (2005).

[14] M. P i e t r z y k, R. K u z i a k, Problem of modelling of deformation materials properties in variable conditions, Computer Methods in Materials Science **2**, 4, 227-258 (2002).

Received: 10 January 2011.